ORIGINAL ARTICLE

Synthesis, structure and property of three divalent metal complexes of the piperidinoacetyl-containing calix[4]arene

Ying-Hua Zhou · Jian Chen · Yong-Jia Shang · Yong Cheng

Abstract Three new mononuclear complexes [Cd(L)] $(ClO_4)_2$·4(MeCN) (**1**) (L = 5,11,17,23-tetra-t-butyl-25,26, 27,28-tetrakis(piperidinocarbonylmethoxy)calix[4]arene), [Zn(L)]$(ClO_4)_2$·4(MeCN)·CH_2Cl_2 (**2**), [Cu(L)]$(ClO_4)_2$·3(MeCN)·Et_2O (**3**) have been synthesized and characterized by elemental analysis and X-ray single crystal diffraction (CCDC: 838342, 838343 and 838344). The results of the crystal structural analyses show that calix[4]arene backbones in **1**, **2**, **3** are fixed in the cone conformation while the divalent metal cations (Cd, Zn and Cu) are coordinated with the discrepant geometry. The cadmium ion in **1** is eight-coordinated with four carbonyl oxygen atoms and four ethereal oxygen atoms in the low rim of calix[4]arene, whereas zinc ion in **2** and copper ion in **1** are four-coordinated with the acyl oxygen atoms. The atomic net charges distribution and frontier molecular orbital energies were obtained by Gaussian 98 program with DFT method at B3LYP/lanl2dz level. Furthermore, the SOD-like activities of **3** were measured by xanthine/xanthine oxidase-NBT assay at pH 7.2 and 7.8.

Keywords Calix[4]arene · Supramolecular chemistry · Complexation · Metalloenzyme model

Y.-H. Zhou (✉) · J. Chen · Y.-J. Shang (✉) · Y. Cheng
Anhui Key Laboratory of Functional Molecular Solids, College of Chemistry and Materials Science, Anhui Normal University, Wuhu 241000, People's Republic of China
e-mail: yhzhou@mail.ahnu.edu.cn

Y.-J. Shang
e-mail: shjy@mail.ahnu.edu.cn

Introduction

Recently, calixarenes derivatives have been extensively applied in the fields of supramolecular architecture, ion sensors, ion transport through liquid membranes, metal extraction and enzyme mimics due to the high preorganization and complementarity with guest molecules and ions [1–6]. Functionalization of calixarenes at the bottom and up rim with the organic groups containing nitrogen, sulfur and oxygen donor atoms represents an effective and versatile way of constructing metal cation receptors or the functional complexes, where the chelating chains can be convergent and interact simultaneously with the coordinated cation. Therefore, the calix[4]arene derivatives can be exploited to effectively scavenge some heavy metals ion pollutants [7–9], or mimic the active site of some metal enzyme. Reinhoudt groups founded that some di-Zn(II) complexes with the calix[4]arene as the hydrolase scaffold behaved the high hydrolytic activity for the ester compounds [10], due to the cooperatively catalytic effect of the two zinc ions. Reinaud and co-worker reported the metal funnel complexes containing the cone conformation of calixarene could mimic the substrate access channel to metalloenzyme active sites because the a variety of guest small molecules/ions were induced and captured by the cavity of calixarene resulting in the spatial favor to the catalysis [11]. Up to the present, the research on the catalytic properties of the metal funnel complex with the cone calixarene is still rare.

Herein, we report the synthesis and structures of the three bivalent metal complexes based on the ligand 5,11,17, 23-tetra-*tert*-butyl-25,26,27,28-tetrakis(piperidinocarbonylmethoxy) calix[4]arene (L), [Cd(L)]$(ClO_4)_2$·4(MeCN) (**1**), [Zn(L)] $(ClO_4)_2$·4(MeCN)·CH_2Cl_2 (**2**), [Cu(L)]$(ClO_4)_2$·3(MeCN)· Et_2O (**3**). The atomic net charges distribution and frontier molecular orbital energies were obtained by Gaussian 98

program with DFT method at B3LYP/LanL2DZ level. Furthermore, the SOD-like activities (SOD = superoxide dismutase) of complex **3** were determined by xanthine/xanthine oxidase-NBT assay.

Experimental section

Materials

All of the chemicals were of analytical reagent grade and were used as received. Organic reagents were reagent grade and redistilled before use. 5,11,17,23-tetra-*tert*-butyl-25,26,27,28-tetrakis(piperidinocarbonylmethoxy)calix[4]arene was synthesized and purified according to literature procedure [12]. Bivalent metallic perchlorate hexahydrate $M(ClO_4)_2 \cdot 6H_2O$ (M = Cd, Zn, Cu) were prepared as our previous work [13, 14].

Measurements

X-ray crystallography

Single-crystal X-ray data of **1**, **2** and **3** was collected on a Bruker Smart Apex CCD diffractometer at 173 K, both with graphite-monochromated Mo Kα radiation (λ) 0.71073 Å. The reflections were corrected for Lorentz and polarization effects, and empirical absorption corrections were applied using the SADABS program [15]. The space groups were determined from systematic absences and confirmed by the results of refinement. The structure of **1**, **2** and **3** was solved by direct methods using the SHELXTL software suite and Sir2004 [16, 17]. All non-hydrogen atoms were refined with anisotropic displacement parameters except some of the disordered ones. All H atoms of the calix[4]arene ligand were placed at idealized positions and refined as riding atoms. Almost all atoms of the metal calix[4]arene complexes were normal, but some atoms of *tert*-butyl group in calix[4]arene exhibited slight disorder. Such disorder situations often appear in the complexes containing *tert*-butyl group [13, 14]. Therefore they do not affect our general understanding the structure of the supramolecular complex. Crystallographic data of **1**, **2** and **3** are listed in Table 1.

SOD activity

Superoxide anion ($O_2^{\bullet-}$) was generated in enzymatic (xanthine/xanthine oxidase) system in the presence or absence of test complexes, and $O_2^{\bullet-}$ production was determined by monitoring the reduction of NBT to monoformazan dye at 560 nm at 25 $\pm$ 0.1 °C [14, 18]. An appropriate amount of xanthine oxidase was added to a mixture of 500 μM NBT, 500 μM xanthine, and 0–1.0 μM complex dissolved in 50 mM phosphate buffer (pH 7.2 and 7.8) to cause a

variation of absorbance ($\Delta A_{560}/\Delta t_{min}$) of 0.025 $\pm$ 0.005. The percentage inhibition (% I) of NBT$^+$ formation was calculated from equation: (%) $I = (A_0 - A_s)/A_0 \times 100$, in which A_0 and A_s are the maximum absorbance values due to NBT$^+$ at 560 nm in the absence and in the presence of the complex. By plotting the % I as a function of complex concentration, the IC$_{50}$ values were calculated.

DFT calculation

The atomic coordinate positions of the complex **1**, **2** and **3** were based on the data of the crystal structures, in which the solvent molecules and equilibrium charge anions ClO_4^- were ignored. DFT calculations with a hybrid functional B3LYP method at the LanL2DZ basis set were performed with Gaussian 98 software package [19]. In **1** and **2**, the charge and multiplicity is respectively set as +2, 1, while +2, 2 with restricted-open spin in **3** because of one unpaired electron in Cu(II). All calculations were performed on a Pentium IV computer using the high convergence criteria. For **1**, 185 atoms, 974 basis functions, 2,536 primitive gaussians, 317 alpha electrons and 317 beta electrons are involved in the calculation. For **2**, 185 atoms, 974 basis functions, 2,539 primitive gaussians, 317 alpha electrons and 317 beta electrons are involved in the calculation. For **3**, 185 atoms, 978 basis functions, 2,552 primitive gaussians, 321 alpha electrons and 320 beta electrons are involved in the calculation.

Preparation of complex 1

To 10 mL acetonitrile solution of L (0.574 g, 0.5 mmol) was slowly added a solution of $Cd(ClO_4)_2 \cdot 6H_2O$ (0.210 g, 0.5 mmol) in 5 mL MeCN with stirring. After 30 min, the mixture solution was filtered and the filtrate was kept at room temperature. The colorless bulk crystals of **1** were isolated after 72 h (yield 46% based on Cd). Mass spectrum MS (ESI, H$_2$O/MeOH, 1:1, v/v, *m/z*): [CdL]$^{2+}$ calcd 631.3, found 631.0. Anal. Calcd. for C$_{80}$H$_{112}$Cl$_2$N$_8$O$_{16}$Cd: C 59.13, N 6.90, H 6.95%; Found: C 59.41, N 7.09, H 6.62%. IR (KBr disc, cm^{-1}): 2944 (m, br), 2859 (w), 1664 (s), 1477 (m), 1403 (s), 1362 (w), 1199 (m), 1127 (w), 1065 (w), 1012 (w), 869 (w). CCDC: 838342.

Preparation of complex 2

To 10 mL dichlormethane solution of L (0.574 g, 0.5 mmol) was slowly added a solution of 5 mL acetonitrile solution of $Zn(ClO_4)_2 \cdot 6H_2O$ (0.186 g, 0.5 mmol). After stirring for 30 min, the mixture solution was filtered and the filtrate was kept at room temperature. The colorless block crystals of **2** were isolated after 36 h (yield 52% based on Zn). Anal. Calcd. for C$_{81}$H$_{114}$Cl$_4$N$_8$O$_{16}$Zn:

Table 1 Crystal data and structure refinement for **1**, **2** and **3**

	1	**2**	**3**
Empirical formula	$C_{80}H_{112}Cl_2N_8O_{16}Cd$	$C_{81}H_{114}Cl_4N_8O_{16}Zn$	$C_{82}H_{118}Cl_2N_7O_{17}Cu$
Formula weight	1,625.08	1,662.97	1,608.27
λ/Å	0.71073	0.71073	0.71073
Temperature/K	173(2)	173(2)	173(2)
Crystal dimensions/mm	$0.12 \times 0.32 \times 0.36$	$0.16 \times 0.45 \times 0.48$	$0.12 \times 0.42 \times 0.48$
Crystal system	Triclinic	Triclinic	Orthorhombic
Space group	P-1	P-1	P2(1)
a/Å	14.580 (3)	14.570 (5)	28.248 (4)
b/Å	15.028 (3)	14.955 (5)	12.970 (2)
c/Å	19.807 (4)	20.016 (4)	22.929 (3)
α/°	86.913 (3)	87.475 (6)	90.00
β/°	80.475 (3)	81.019 (7)	90.00
γ/°	77.675 (3)	77.676 (6)	90.00
V/Å^3	4,180.7 (13)	4,208.37 (75)	8,400.65 (27)
Z	2	2	4
D_c/Mg m^{-3}	1.291	1.312	1.272
Absorpt. coeff μ/mm^{-1}	0.392	0.487	0.392
F (000)	1,716	1,764	3,432
θ Range/°	1.72–27.12	1.03–27.18	1.44–26.09
Reflections collected	35,107	35,898	38,593
Independent reflections	1,7965 [$R_{int} = 0.0437$]	1,8203 [$R_{int} = 0.0339$]	1,4382 [$R_{int} = 0.0957$]
R_1 ($I > 2\sigma(I)$)[a]	0.0594	0.0636	0.1500
wR_2 (all data)[b]	0.1564	0.1762	0.3507
Goodness-of-fit on F^2	1.062	1.044	1.370
$\Delta\rho_{max, min}$/e Å^{-3}	1.117, −0.726	0.672, −1.094	4.555, −1.741

[a] $R_1 = \sum ||F_0| - |F_C||/\sum |F_0|$

[b] $wR_2 = \sum [w(F_0^2 - F_C^2)^2]/\sum [w(F_0^2)^2]^{1/2}$

C 58.50, N 6.91, H 6.74%; Found: C 58.72, N 7.12, H 6.54%. CCDC: 838343.

Preparation of complex 3

To 10 mL acetonitrile containing L (0.574 g, 0.5 mmol) was slowly added a solution of 5 mL acetonitrile solution of $Cu(ClO_4)_2 \cdot 6H_2O$ (0.185 g, 0.5 mmol). After stirring for 30 min, the mixture solution was filtered. Then the filtrate was diffused in the ethyl ether at 4 °C. The blue plate crystals of **3** were isolated after 120 h (yield 41% based on Cu). Anal. Calcd. for $C_{82}H_{118}Cl_2N_7O_{17}Cu$: C 61.24, N 6.10, H 7.40%; Found: C 61.46, N 6.38, H 7.21%. CCDC: 838344.

Results and discussion

Crystal structure analysis

The coordination environment of metal cations and the selected bond lengths of **1**, **2** and **3** are illustrated in Figs. 1,

2, 3. Single-crystal X-ray diffraction analysis reveals that **1**, **2** and **3** consist of perchlorate anions, solvent molecules and a metal-calix[4]arene unit, in which metal cations (Cd^{2+}, Zn^{2+} and Cu^{2+}) are coordinated to the oxygen atoms located at the bottom rim of calix[4]aren. The cadmium geometry in **1** (Fig. 1) is described as a distorted square antiprism, in which the metal cation is coordinated by eight oxygen atoms with four acyl oxygen atoms and four phenol oxygen atoms of calix[4]arene. Obviously, the nitrogen atoms of piperidino groups have not been coordinated to the cadmium ion, although the nitrogen atom has a more compatibility to a soft metal cation than the oxygen atom. It may be contributed to the fact that the lower rim with piperidinoacetyl groups is capacious so that the nitrogen atoms of four piperidino groups are far enough not to be coordinated to metal cation. The ethereal and acyl oxygen atoms lay on the two discrete *quasi*-parallel squares planes, which are about 2.275 Å apart and tilted 0.839° from each other. The Cd(II) cation is sandwiched between the two bases and is slight closer to the ethereal oxygen plane (1.101 (4) Å) than to the acyl oxygen plane (1.174

Fig. 1 Coordination environment of the Cd(II) atom in **1** (**a** *side view*, **b** *top view*). All of the solvent molecules, perchlorate anions and hydrogen atoms are omitted for clarity. Selected bond lengths (Å): Cd(1)–O(1) 2.434(3), Cd(1)–O(5) 2.365(3), Cd(1)–O(2) 2.447 (3), Cd(1)–O(6) 2.270 (3), Cd(1)–O(3) 2.455 (3), Cd(1)–O(7) 2.369 (3), Cd (1)–O(4) 2.486(3), Cd(1)–O(8) 2.267 (3)
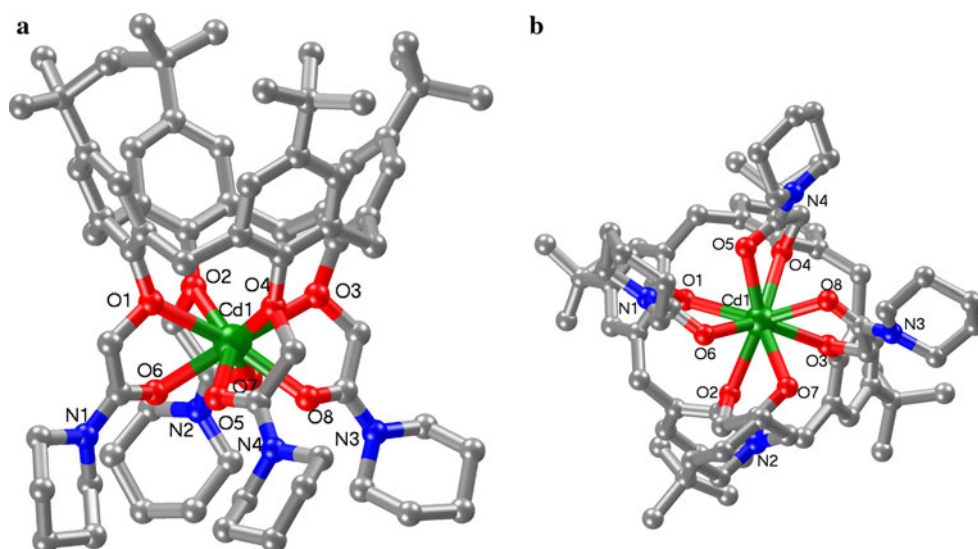
(4) Å). The bond lengths of Cd–O of the ethereal and acyl oxygen are in the range of 2.434 (2)–2.486 (3) Å and 2.267 (3)–2.369 (3) Å, respectively, which are typical for the Cd–O complexes [20–22]. In **1**, the cadmium cation is charge-balanced by two perchlorate anions. Moreover, there are also four isolated acetonitrile solvent molecules co-crystallized with the calixarene. In the packing arrangement, the complex **1** are packed together with perchlorate anions and isolated acetonitrile molecules via the electrostatic forces and H-bonding interactions to form a supramolecular framework. As far as **2** and **3** is concerned, the coordination environments around the metal cation are similar. The complexation geometry in **2** (Fig. 2) and **3** (Fig. 3) are described as the distorted tetragonal pyramid, in which the zinc or copper cation is coordinated by the four acyl oxygen atoms at the low rim of calix[4]arene. Unlike the cadmium complex **1**, the phenol ethereal oxygen atoms

in **2** and **3** have not been coordinated, due to the fact that the distances between the metal ion and ethereal oxygen atoms (Zn–O, 2.4633 (5), 2.4763 (5), 2.5131 (5), 2.6183 (5) Å; Cu–O, 2.7937 (3), 2.8607 (4), 3.1035 (4), 3.1967 (4) Å, respectively) obviously exceed the normal range of the bonds Zn–O and Cu–O [23, 24]. In **2** and **3**, the acyl oxygen atoms lay on the *quasi*-squares planes, in which the torsion angle is 9.306 and 2.941°, respectively. The distance from the metal ion to the plane of the carbonyl oxygens is 0.957 Å for **2**, and 0.419 Å for **3**. The bond lengths of Zn–O in the carbonyl oxygens plane are in the range from 2.037 (2) to 2.223 (3) Å, which are typical for the ZnO_4 complexes [23]. And the bond lengths of Cu–O are in the range 1.910 (10)–1.937 (10) Å, which can be matched to the bond distance of the copper complex [24]. In **2** and **3**, the two perchlorates ions and the space filling solvent molecules are in the periphery of the complexes at interstitial lattice sites,

Fig. 2 Coordination environment of the Zn(II) atom in **2** (**a** *side view*, **b** *top view*). All of the solvent molecules, perchlorate anions and hydrogen atoms are omitted for clarity. Selected bond lengths (Å): Zn(1)–O(5) 2.223 (3), Zn(1)–O(6) 2.037 (2), Zn(1)–O(7) 2.173 (2), Zn(1)–O(8) 2.055 (2)
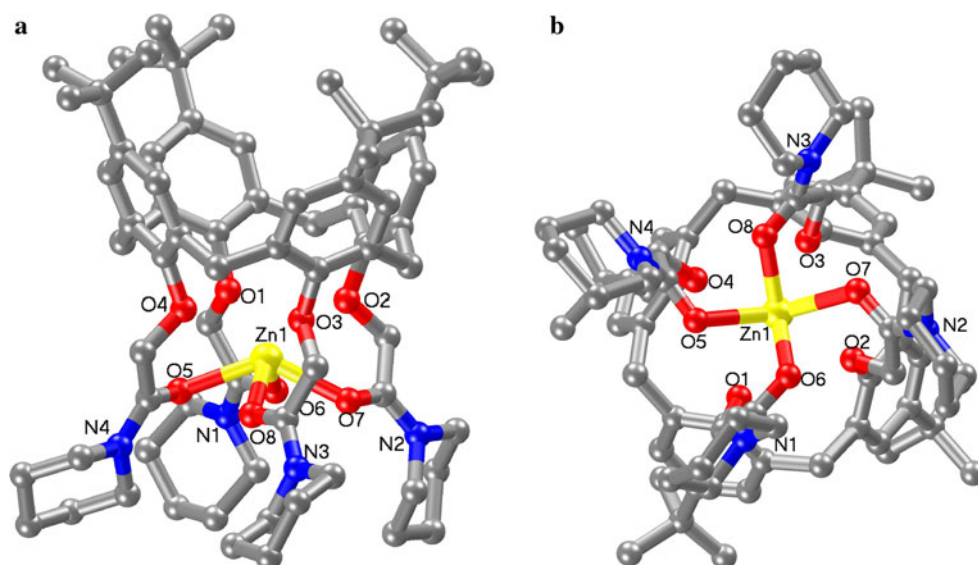
Fig. 3 Coordination environment of the Cu(II) atom in **3** (**a** *side view*, **b** *top view*). All of the solvent molecules, perchlorate anions and hydrogen atoms are omitted for clarity. Selected bond lengths (Å): Cu(1)–O(1) 1.937 (10), Cu(1)–O(3) 1.910 (10), Cu(1)–O(5) 1.914 (9), Cu(1)–O(7) 1.928 (9)
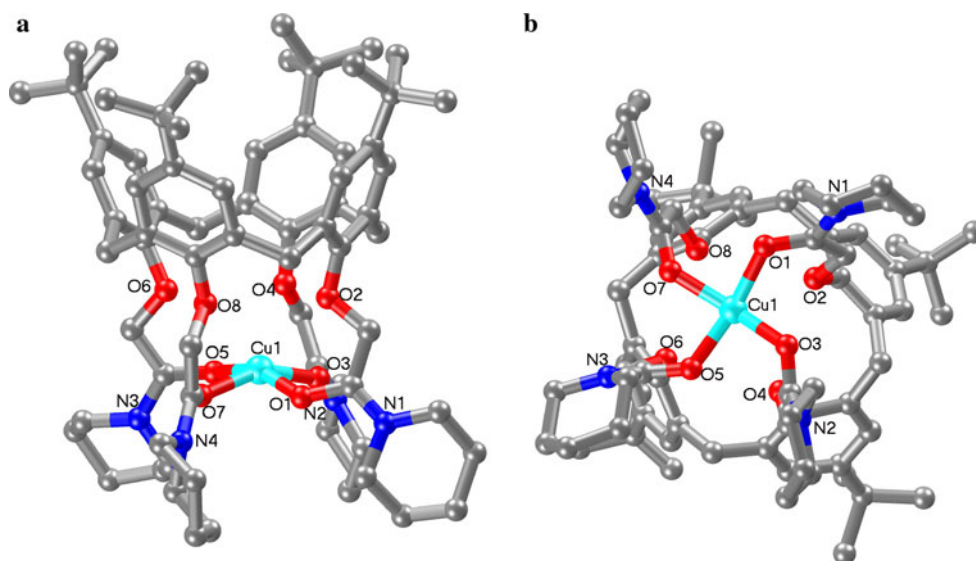
Table 2 Dihedral angles in **1**, **2** and **3**

	1	**2**	**3**
τ_1 (°)	141.20 (13)	140.38 (9)	102.40 (27)
τ_2 (°)	108.77 (13)	127.34 (8)	99.26 (30)
τ_3 (°)	139.13 (13)	109.10 (7)	103.04 (29)
τ_4 (°)	109.64 (14)	97.57 (10)	93.56 (26)
$\angle(ph_1, ph_3)$ (°)	45.37 (14)	61.80 (7)	45.68 (30)
$\angle(ph_2, ph_4)$ (°)	69.43 (15)	68.96 (10)	50.82 (32)

in **2** four isolated acetonitrile and one dichlormethane molecules, while in **3** three isolated acetonitrile and one ethyl ether molecules.

As a result of the metal cation interaction with the bottom rim of **1**, **2** and **3**, the calixerenes are shaped by the four-phenyl rings adopt a relatively open distorted cone conformation which can be described by the dihedral angles (τ) that the phenol rings subtend with the plane through the four CH$_2$ linking groups. For the sake of comparison, the τ-values of **1**, **2** and **3** are listed in Table 2, in which the obtuse τ-values indicate phenyl rings are tilted so that their *tert*-butyl groups are pitched away from the open cavity. This table also includes the interplanar angles, $<$(ph1, ph3) and $<$(ph2, ph4), between pair of opposite phenyl rings. These crystallographic data indicate that the piperidinoacetyl-containing calix[4]arene has a stronger binding ability for the divalent metal cations.

Table 3 Mulliken atomic charges of part atoms of complex at the B3LYP/LanL2DZ level
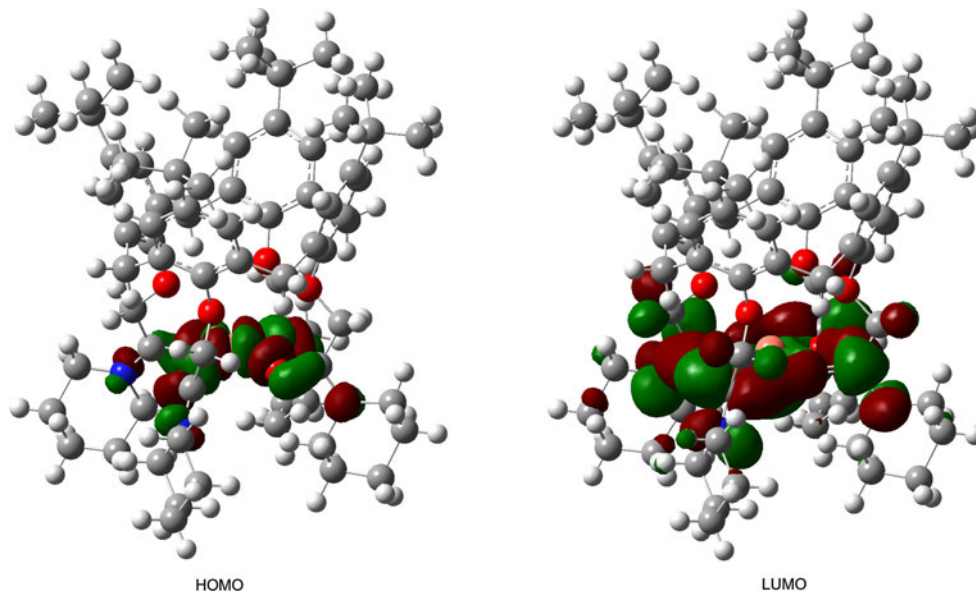
1		**2**		**3**	
Atom	Charge	Atom	Charge	Atom	Charge
Cd1	1.064357	Zn1	0.999623	Cu1	0.596489
O1	−0.443316	O1	−0.403936	O1	−0.450951
O2	−0.444375	O2	−0.417794	O2	−0.341625
O3	−0.432657	O3	−0.396398	O3	−0.404515
O4	−0.435437	O4	−0.390346	O4	−0.348714
O5	−0.399212	O5	−0.414767	O5	−0.431490
O6	−0.415589	O6	−0.456155	O6	−0.334219
O7	−0.407618	O7	−0.425211	O7	−0.408557
O8	−0.405319	O8	−0.447010	O8	−0.327565
N1	−0.109135	N1	−0.104365	N1	−0.092153
N2	−0.104684	N2	−0.104607	N2	−0.135112
N3	−0.113830	N3	−0.110718	N3	−0.125172
N4	−0.106446	N4	−0.107850	N4	−0.097569

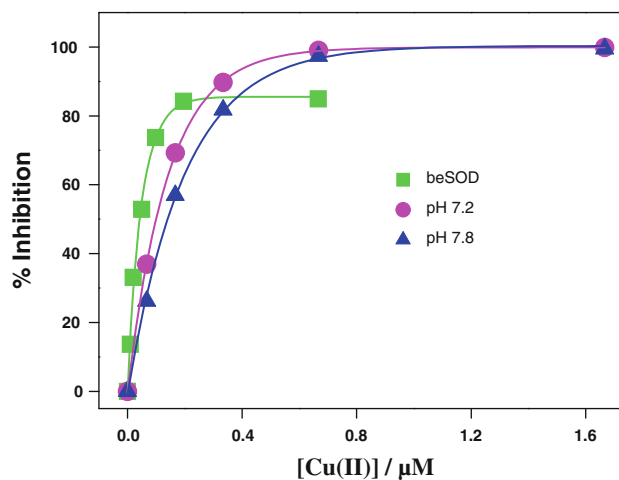**Table 4** Frontier molecular orbital energies (eV) of complex at the B3LYP/LanL2DZ level

Energies (eV)	1	2	3
HOMO	−10.0622	−9.4044	−7.0378
LUMO	−4.6293	−4.8865	−5.6298
ΔE	5.4329	4.5179	1.40780

DFT calculation analysis

By the analysis of Mulliken population, some information of atom net charges were obtained (Table 3), in which the net charge of M(II) (M = Cd, Zn and Cu) is less than the original value (+2). In **2**, the net negative charge of O5–O8 are higher than that of O1–O4 and N1–N4, suggesting that zinc ion was preferentially coordinated by the four acyl oxygen atoms. For **3**, the net negative charge of O1, O3, O5 and O7 are higher than that of other O and N atoms, implied that phenol ethereal oxygen and piperidino nitrogen atoms did not take part in the metal complexation. The frontier molecular orbital energies of the complexes are listed in Table 4, where the occupied molecular orbital energies are all negative, indicating the complex is stable. Compared with **1** and **2**, the energy difference ($\Delta E = E$LUMO − EHOMO) of **3** is relatively lower, suggesting

Fig. 5 Percentage of inhibition of superoxide radicals formed by xanthine/xanthine oxidase enzyme assayed by NBT$^+$ absorption at 560 nm in the presence of bovine erythrocyte SOD at pH = 7.8 (*filled square*), **3** at pH = 7.8 (*filled triangle*), and **3** at pH = 7.2 (*filled circle*) (500 μM xanthine, 0.04 unit of xanthine oxidase and 500 μM NBT, 0.1 M phosphate buffer)

the strong activity of the copper complex. As shown in Fig. 4 and Table 5, the copper atomic orbital contribution to the highest occupied molecular orbital and lowest unoccupied molecular orbital of **3** is greater than other atoms, which indicate that copper atom has the potential of

Fig. 4 Schematic diagram of the frontier MO for the complex **3**

HOMO

LUMO

Table 5 Some atomic orbital contribution to frontier molecular orbitals (%) of **3**

MO	Cu1	O1	O2	O3	O4	O5	O6	O7	O8
HOMO	66.3013	6.3816	0.0042	5.7937	0.0079	5.2222	0.0218	5.3904	0.0068
LUMO	5.3221	2.4557	0.0205	1.8034	0.0082	1.5500	0.0599	1.3318	0.0120

Table 6 SOD activities (IC$_{50}$ values) of model complexes and native Cu$_2$, Zn$_2$−SOD

| Complexes	IC$_{50}$ (μM)	References
3	0.14	This work
3[a]	0.10	This work
[Cu(bbda)(H$_2$O)$_2$(βCD)]$^{2+}$	0.17	[14]
Native Cu$_2$,Zn$_2$-SOD	0.04	[28]
[Cu$_2$(bbda)(im)(H$_2$O)$_2$(βGCD)]$^{2+}$	0.20	[29]
[CuZn(Me$_4$bdpi)(H$_2$O)$_2$]$^{3+}$	0.24	[30]
[Cu$_2$(Me$_4$bdpi)(H$_2$O)$_2$]$^{3+}$	1.1	[30]
[Cu$_2$(bpzbiap)Cl$_3$]	0.52	[31]

[a] pH 7.2, other pH 7.8

bbda 4-(4′-tert-butyl-benzyl)diethylenetriamine, *Me$_4$bdpi* 4,5-bis(di-(6-methyl-2-pyridylmethyl)aminomethyl)imidazolate, *Hbpzbiap* 1,5-bis(1-pyrazolyl)-3-[bis(2-imidazolyl)methyl]azapentane

accepting lone electron pair of $O_2^{\bullet-}$ as an active center, and therefore it has the antioxidative activity [25].

SOD-like activity

The SOD-like activities of **3** were investigated by xanthine/xanthine oxidase-NBT assay [26, 27]. As shown in Fig. 5, the measured IC$_{50}$ value of bovine erythrocyte SOD is 0.042 ± 0.01 μM, being almost identical to 0.04 μM value reported [28]. The calixarene derivative did not exhibit $O_2^{\bullet-}$ scavenger effects under the same conditions. As seen from the Table 6, the activity of **3** exhibited a remarkably higher SOD-like activity (IC$_{50}$ = 0.14 μM) at pH 7.8 than those of the SOD mimics previously described in the literatures [29–31]. Moreover, the SOD-like activity of **3** at pH 7.2 enhanced by about 30% in comparison with at pH 7.8. It

Scheme 1 A schematic diagram of the suggested $O_2^{\bullet-}$ dismutation reaction catalyzed by **3**
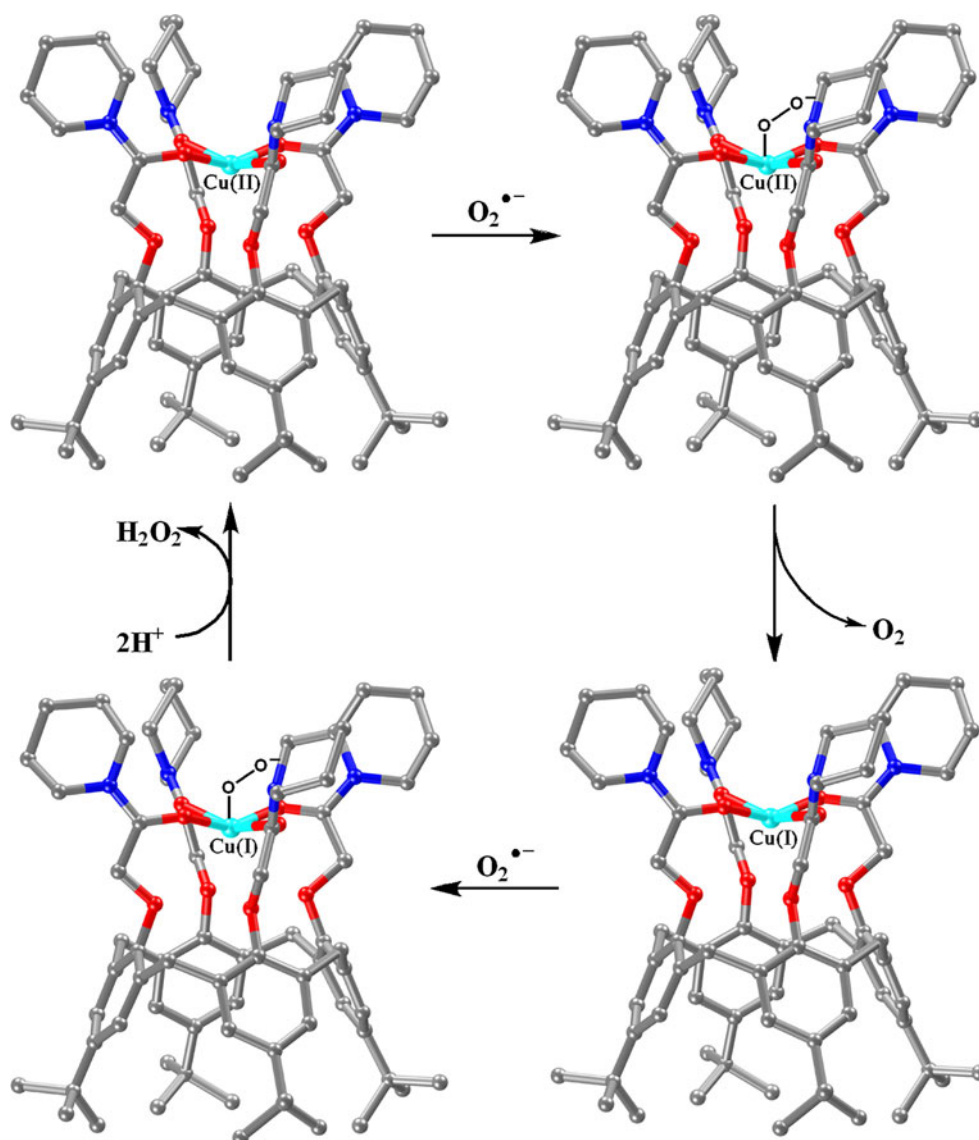
may be ascribed to the introduction of the second coordination surrounding provided by the piperidinoacetyl-containing calixarene derivative, in which the hydrophobic cavity serves as the channels of the small molecular substrate and the protonated piperidyl groups electrostatically steer the superoxide anion to/from the active copper ion. This result strongly supported that the protonated piperidyl groups around copper center afford the extra driving forces for the superoxide anion, similar to the Arg function around the active site in the nature Cu_2, Zn_2-SOD [32]. On the basis of above results and early suggested catalytic mechanisms [33, 34], a possible mechanism for catalytic process is proposed as Scheme 1. Firstly, a superoxide anion is attracted and then bonded by the Cu(II) ion. Secondly, the superoxide anion releases its electron directly to the Cu(II) ion and then the forming electrically neutral oxygen molecule leaves. Thirdly, second superoxide anion is attracted is attracted and then bonded by the Cu(I) ion. Fourthly, the superoxide anion accepts an electron and further combines two protons from the solution forming a H_2O_2 molecule. The catalytic cycle was achieved after releasing the electrically neutral hydrogen peroxide.

Conclusion

In summary, the crystal structures of the new three bivalent metal (Cd, Zn, Cu) complexes **1**, **2**, **3** based on the piperidinoacetyl-containing calix[4]arene have reveal the discrepant coordination conformations, which are helpful to design and construct the calixarene-based mimics and ion-sensors. The complex **3** exhibits the high SOD-like activity due to the introduction of the hydrophobic cavity and the protonated piperidyl groups. It maybe provide a new strategy for the design of the metalloenzyme models.

Supplementary material

Crystallographic data (excluding structure factors) for the structures in this article have been deposited with the Cambridge Crystallographic Data Centre with supplementary publication numbers CCDC 838342, 838343 and 838344. These data can be obtained free of charge from the CCDC, E-mail: deposit@ccdc.cam.ac.uk.

References

1. Mutihac, L.: Calix[n]arenes as synthetic membrane transporters: a minireview. Anal. Lett. **43**, 1355–1366 (2010)
2. Perret, F., Coleman, A.W.: Biochemistry of anionic calix[n]arenes. Chem. Commun. **47**, 7303–7319 (2011)
3. Cacciapaglia, R., Casnati, A., Mandolini, L., Reinhoudt, D.N., Salvio, R., Sartori, A., Ungaro, R.: Catalysis of diribonucleoside monophosphate cleavage by water soluble copper(II) complexes of calix[4]arene based nitrogen ligands. J. Am. Chem. Soc. **128**, 12322–12330 (2006)
4. Izzet, G., Douziech, E., Prange, T., Tomas, A., Jabin, I., Le Mest, Y., Reinaud, O.: Calix[6]tren and copper(II): a third generation of funnel complexes on the way to redox calix-zymes. Proc. Natl. Acad. Sci. USA **102**, 6831–6836 (2005)
5. Ikeda, A., Shinkai, S.: Novel cavity design using calix[n]arene skeletons: Toward molecular recognition and metal binding. Chem. Rev. **97**, 1713–1734 (1997)
6. Wang, G.-S., Zhang, H.-Y., Ding, F., Liu, Y.: Preparation and characterization of inclusion complexes of topotecan with sulfonatocalixarene. J. Incl. Phenom. Macro. **69**, 85–89 (2011)
7. de Namor, A.F.D., Chahine, S., Kowalska, D., Castellano, E.E., Piro, O.E.: Selective interaction of lower rim calix[4]arene derivatives and bivalent cations in solution. Crystallographic evidence of the versatile behavior of acetonitrile in lead(II) and cadmium(II) complexes. J. Am. Chem. Soc. **124**, 12824–12836 (2002)
8. Guo, D.-S., Wang, K., Liu, Y.: Selective binding behaviors of p-sulfonatocalixarenes in aqueous solution. J. Incl. Phenom. Macro. **62**, 1–21 (2008)
9. Wang, L., Li, H., Jiang, Z., Gu, J., Shi, X.: The synthesis of nitrogen-containing calixarene derivatives and their interactions with lead ions. J. Incl. Phenom. Macro. **42**, 39–43 (2002)
10. Cacciapaglia, R., Casnati, A., Mandolini, L., Peracchi, A., Reinhoudt, D.N., Salvio, R., Sartori, A., Ungaro, R.: Efficient and selective cleavage of RNA oligonucleotides by calix[4]arene-based synthetic metallonucleases. J. Am. Chem. Soc. **129**, 12512–12520 (2007)
11. Le Poul, N., Douziech, B., Zeitouny, J., Thiabaud, G., Colas, H., Conan, F., Cosquer, N., Jabin, I., Lagrost, C., Hapiot, P., Reinaud, O., Le Mest, Y.: Mimicking the protein access channel to a metal center: Effect of a funnel complex on dissociative versus associative copper redox chemistry. J. Am. Chem. Soc. **131**, 17800–17807 (2009)
12. Bocheńska, M., Banach, R., Zielińska, A., Kravtsov, V.C.H.: Lower rim substituted tert-butyl calix[4]arenes (I). The structure and complexing properties in ion-selective PVC membrane electrodes. J. Incl. Phenom. Macro. **39**, 219–228 (2001)
13. Zhou, Y.H., Fu, H., Zhao, W.X., Tong, M.L., Su, C.Y., Sun, H., Ji, L.N., Mao, Z.W.: An effective metallohydrolase model with a supramolecular environment: Structures, properties, and activities. Chem. Eur. J. **13**, 2402–2409 (2007)
14. Zhou, Y.H., Fu, H., Zhao, W.X., Chen, W.L., Su, C.Y., Sun, H., Ji, L.N., Mao, Z.W.: Synthesis, structure, and activity of supramolecular mimics for the active site and arg141 residue of copper, zinc-superoxide dismutase. Inorg. Chem. **46**, 734–739 (2007)
15. Sheldrick, G.M.: SADABS, program for scaling and correction of area detector data. University of Göttingen, Göttingen (1996)
16. Sheldrick, G.M.: Shelxs-97, program for crystal structure solution. University of Göttingen, Göttingen (1997)
17. Sheldrick, G.M.: Shelxl-97, program for crystal structure refinement. University of Göttingen, Göttingen (1997)
18. Schepetkin, I., Potapov, A., Khlebnikov, A., Korotkova, E., Lukina, A., Malovichko, G., Kirpotina, L., Quinn, M.: Decomposition of reactive oxygen species by copper(II) bis(1-pyrazolyl)methane complexes. J. Biol. Inorg. Chem. **11**, 499–513 (2006)

19. Frisch, M.J., Trucks, G.W., Schlegel, H.B., Scuseria, G.E., Robb, M.A., Cheeseman, J.R., Zakrzewski, V.G., Montgomery, J.A.Jr., Stratmann, R.E., Burant, J.C., Dapprich, S., Millam, J.M., Daniels, A.D., Kudin, K.N., Strain, M.C., Farkas, O., Tomasi, J., Barone, V., Cossi, M., Cammi, R., Mennucci, B., Pomelli, C., Adamo, C., Clifford, S., Ochterski, J., Petersson, G.A., Ayala, P.Y., Cui, Q., Morokuma, K., Malick, D.K., Rabuck, A.D., Raghavachari, K., Foresman, J.B., Cioslowski, J., Ortiz, J.V., Baboul, A.G., Stefanov, B.B., Liu, G., Liashenko, A., Piskorz, P., Komaromi, I., Gomperts, R., Martin, R.L., Fox, D.J., Keith, T., Al-Laham, M.A., Peng, C.Y., Nanayakkara, A., Gonzalez, C., Challacombe, M., Gill, P.M.W., Johnson, B., Chen, W., Wong, M.W., Andres, J.L., Gonzalez, C., Head-Gordon, M., Replogle, E.S., Pople, J.A.: Gaussian 98, Revision A. 7. Gaussian, Inc., Pittsburgh (1998)

20. Wang, X., Li, L., Hou, H., Wu, J., Fan, Y.: Substitution, addition, and recombination reactions of precursor complexes with ferrocenyl carboxylate units. Eur. J. Inorg. Chem. **2007**, 5234–5245 (2007)

21. Hines, C.C., Reichert, W.M., Griffin, S.T., Bond, A.H., Snowwhite, P.E., Rogers, R.D.: Exploring control of cadmium halide coordination polymers via control of cadmium(II) coordination sites utilizing short multidentate ligands. J. Mol. Struct. **796**, 76–85 (2006)

22. Zhou, X.-Y., Huang, Y.-Q., Sun, W.-Y.: Syntheses, structures and photoluminescent property of coordination complexes with 2-(1H–1,2,4-triazol-1-yl)acetic acid. Inorg. Chim. Acta **362**, 1399–1404 (2009)

23. Dong, W., Li, G., Shi, Z., Fu, W., Zhang, D., Chen, X., Dai, Z., Wang, L., Feng, S.: Hydrothermal synthesis and structural characterization of an organically-templated zincophosphite: $[C_4N_2H_{12}]_{0.5} \cdot [Zn_3(HPO_3)_4] \cdot H_3O$. Inorg. Chem. Commun. **6**, 776–780 (2003)

24. RodrIguez-MartIn, Y., Lorenzo Luis, P.A., Ruiz-Pérez, C.: Extended network via hydrogen bond linkages of coordination compounds: synthesis, crystal structure and thermal behaviour of the complexes $[M(L)_2(NO_3)_2]$ (MII = Cu, Co) and $[Ni(L)_2(H_2O)_2]$ $[(NO_3)_2]$ (L = malonamide). Inorg. Chim. Acta **328**, 169–178 (2002)

25. Zhao, R., Liu, X.-H., Yin, Y.-X., Yue, J.-J., Sun, Y., Ma, Y., Liu, X.-L.: Quantum chemistry calculation of the copper and zinc active site of natural enzyme. Chin. J. Org. Chem. **23**, 1001–1003 (2003)

26. Beauchamp, C., Fridovich, I.: Superoxide dismutase: improved assays and an assay applicable to acrylamide gels. Anal. Biochem. **44**, 276–287 (1971)

27. Serbest, K., Özen, A., Ünver, Y., Er, M., Degirmencioglu, I., Sancak, K.: Spectroscopic and theoretical study of 1,2,4-triazole-3-one based salicylaldimine complexes and evaluation of superoxide-scavenging properties. J. Mol. Struct. **922**, 1–10 (2009)

28. Weser, U., Schubotz, L.M., Lengfelder, E.: Imidazole-bridged copper complexes as Cu_2Zn_2-superoxide dismutase models. J. Mol. Catal. **13**, 249–261 (1981)

29. Fu, H., Zhou, Y.H., Chen, W.L., Deqing, Z.G., Tong, M.L., Ji, L.N., Mao, Z.W.: Complexation, structure, and superoxide dismutase activity of the imidazolate-bridged dinuclear copper moiety with beta-cyclodextrin and its guanidinium-containing derivative. J. Am. Chem. Soc. **128**, 4924–4925 (2006)

30. Ohtsu, H., Shimazaki, Y., Odani, A., Yamauchi, O., Mori, W., Itoh, S., Fukuzumi, S.: Synthesis and characterization of imidazolate-bridged dinuclear complexes as active site models of Cu,Zn-SOD. J. Am. Chem. Soc. **122**, 5733–5741 (2000)

31. Tabbì, G., Driessen, W.L., Reedijk, J., Bonomo, R.P., Veldman, N., Spek, A.L.: High superoxide dismutase activity of a novel, intramolecularly imidazolato-bridged asymmetric dicopper(II) species. Design, synthesis, structure, and magnetism of copper(II) complexes with a mixed pyrazole–imidazole donor set. Inorg. Chem. **36**, 1168–1175 (1997)

32. Banci, L., Bertini, I., Luchinat, C., Hallewell, R.A.: An investigation of superoxide dismutase Lys-143, Ile-143, and Glu-143 mutants: Cu_2Co_2SOD derivatives. J. Am. Chem. Soc. **110**, 3629–3633 (1988)

33. Hart, P.J., Balbirnie, M.M., Ogihara, N.L., Nersissian, A.M., Weiss, M.S., Valentine, J.S., Eisenberg, D.: A structure-based mechanism for copper-zinc superoxide dismutase. Biochemistry **38**, 2167–2178 (1999)

34. Ellerby, L.M., Cabelli, D.E., Graden, J.A., Valentine, J.S.: Copper-zinc superoxide dismutase: why not ph-dependent? J. Am. Chem. Soc. **118**, 6556–6561 (1996)